INTERGRANULAR AND INTERPHASE BOUNDARIES IN MATERIALS

Interface controlled active fracture modes in glass-ceramics

Panagiotis Kavouras · Thomas Kehagias ·
Philomela Komninou · Konstantinos Chrissafis ·
Constantine Charitidis · Theodoros Karakostas

Abstract The active fracture modes in glass-ceramics, produced by controlled crystallization from three starting vitreous products containing PbO and SiO_2, were studied and compared. The goal was to examine the active fracture modes in PbO-rich glass-ceramic materials, where the main glass former was PbO, and compare these results with those reported in the literature, where the main glass former was SiO_2. The influence of composition, shape and mean size of the ceramic phase on the active fracture modes of the glass-ceramics was also examined. It was observed that the microhardness and fracture toughness of the starting vitreous products decrease with increasing PbO content. Increase in the relative amount of SiO_2 resulted in a decrease of the percentage of the ceramic phase. Glass-ceramics with higher PbO content showed typical behaviour of high toughness material, i.e. intergranular fracture mode, with lower microhardness value. Glass-ceramics with lower PbO content showed typical behaviour of high-strength material, i.e. transgranular fracture mode, with higher microhardness value.

P. Kavouras · T. Kehagias (✉) · P. Komninou · K. Chrissafis ·
T. Karakostas
Department of Physics, Aristotle University of Thessaloniki,
541 24 Thessaloniki, Greece
e-mail: kehagias@auth.gr

C. Charitidis
School of Chemical Engineering, National Technical University
of Athens, 9 Heroon Polytechniou St., Zographos,
157 80 Athens, Greece

Introduction

The production of glass-ceramics is based on the controlled devitrification of vitreous materials. The batch composition and devitrification conditions determine the morphological characteristics of the end-products. Glass-ceramic materials draw significant scientific interest, mainly during last decades. The reason is that they have a wide variety of applications, since they combine high flexural strength, significant fracture toughness, translucency and casting without the development of pores [1]. They also possess a large number of morphological characteristics, which affect their mechanical performance. Since the conditions of devitrification determine these morphological characteristics, the mechanical performance can be tailored according to the requirements of the final application (e.g. structural materials, armours) rendering glass-ceramics versatile.

It has been recently shown that composition and morphological properties such as, shape and mean size of the ceramic phase strongly affect the active fracture modes in a glass-ceramic material [2]. The above morphological properties can be tailored in a relatively easy manner, by controlling the devitrification conditions or/and the composition of the parent vitreous products. As a result, the final mechanical performance of the glass-ceramic product, namely whether it will have the characteristics of high strength or toughness can be controlled by tailoring the morphology of the final glass-ceramic product.

The general consensus is that in glass-ceramics with weakened interfaces between separated crystallites and the residual amorphous matrix, the active fracture mode is intergranular promoting toughening [3]. In glass-ceramic materials with stronger interfaces, the active fracture mode is transgranular promoting strengthening, similarly to

ceramic materials [4]. The above argument can support the observation that crystallites of different composition can cause different fracture modes, since the crystallite/amorphous matrix interface bears different energy per unit area. It can also support the observation that a change in the crystallites' morphology can have the same effect. Namely, granular-shaped and needle-shaped crystallites of the same composition may produce different fracture modes, since the former have less specific area of interfaces compared to the latter.

However, in has been reported that decrease in the crystallites' mean size, without any modification in the composition or shape results in a shift of the fracture mode, from intergranular to transgranular. Since the composition of the crystallite and the residual amorphous matrix is constant, the strength of cohesion of the crystallite/amorphous matrix interface is also constant. Therefore, it was assumed that in such cases the most important parameter is the size of the crystalline inclusions with respect to the width of a disordered zone acting as an interface between them and the amorphous matrix [5].

In the present study, three glass compositions based on lead oxide, with additions of silica, were devitrified and the resulting glass-ceramic products were produced by controlled devitrification. The motivation behind this work was to examine whether the assumptions and results obtained on silicate glass-ceramics [2, 5], where the vitreous network is composed of Q_4 and Q_3 SiO_4 structural units [6], are valid in glass-ceramic materials, where the vitreous network is composed of PbO_4/PbO_3 structural units [7]. More specifically, the effect of shape and composition of separated crystallites on the fracture mode was studied.

Experimental

In Table 1, the batch compositions of the parent glasses and the elemental compositions of the glass samples obtained by Energy Dispersive Spectrometry (EDS) are listed. All starting materials were in oxide form. After weighting, all batch components were milled in a Fritsch Pulverisette "O" vertically vibrating ball milling apparatus, in order to obtain a homogeneous solid mixture. The solid mixtures were put in platinum crucible and all batch components were subsequently co-melted in a Nabertherm electric furnace in air for 30 min at temperatures listed in Table 1. Relatively low melting temperatures and short melting duration were selected in order to reduce loss of PbO due to evaporation. The homogenized melts were poured on a stainless steel plate and quenched in the form of solid droplets.

Glass-ceramic samples were produced by single-stage thermal treatment of the parent glasses. Thermal treatment

temperatures are also listed in Table 1. These temperatures were chosen based on the results of Differential Thermal Analysis (DTA), i.e. near the exotherms of the respective DTA scans, since in most cases exotherms correspond to crystal phase separation. As a result, thermal treatment at temperatures near possible crystallization temperatures will easily give rise to crystallization of the parent vitreous products.

All as-quenched products were subjected to DTA and EDS characterization. DTA was applied in order to find the glass transition temperature and exothermic peaks, as already mentioned. EDS analyses were performed in order to inspect the elemental homogeneity of the as-quenched products. Namely, 20 analyses were made in each sample on flat and polished surfaces, and the fluctuation in the composition of the constitutive elements was compared with the sensitivity of the method (namely ±1 wt.%).

The microhardness of all products was measured by the static microindentation technique, using Knoop diamond indenter geometry (H_K). The indentation fracture toughness (K_{IC}) was obtained by measuring the length of the median crack system produced on the surface of the samples from the indentation of a Vickers diamond indenter applying the equation [8, 9]:

$$K_{IC} = \delta(E/H_K)^{1/2}(P/c)^{3/2}, \tag{1}$$

where E is the elastic modulus, P the indentation load, c the crack length, and δ a constant with a value of 0.016 for a Vickers indenter geometry. The above measurements were made by obtaining 20 indentations that produced isotropic microcrack propagation, i.e. the microcracks should be emanating from all four corners of the indentation prints. The elastic modulus was calculated from the equation [10]:

$$d/D = (1/7.11) - 0.45(H_K/E), \tag{2}$$

where d and D are the smaller and longer diagonals of a Knoop indentation print, respectively.

The modes of fracture were determined by observing the paths of crack propagation with respect to the crystallite/amorphous matrix interfaces by optical microscopy. Cracks were produced on mechanically polished flat surfaces of the thermally treated products with a Vickers diamond indenter. An Anton-Paar MHT-10 microhardness tester attached on a Zeiss Axiolab-A optical microscope was utilized. The load for Knoop indentations was 1.2 N, for all specimens. This load is high enough so as the obtained microhardness value to lie on the plateau region of the indentation size effect curve. The indentation duration of 10 s is a typical time that is long enough for the onset of plasticity.

In the case of Vickers indentations, the load range was selected to produce indentations with clearly defined radial

Table 1 Batch and EDS derived compositions of the parent vitreous products and the corresponding annealing conditions in order to acquire glass-ceramics

Code name	T_m (°C)	Batch composition (wt.%)		EDS elemental composition (wt.%)		Thermal treatment		Ceramic phase composition
		PbO	SiO$_2$	PbO	SiO$_2$	T (°C)	t (min)	
9/1	850	90	10	85.2	14.8	450	30	Pb$_4$SiO$_6$
8/2	850	80	20	81.0	19.0	550	30	Pb$_3$Si$_2$O$_7$
7/3	900	70	30	72.9	27.1	550	30	Pb$_3$Si$_2$O$_7$

cracks from all four corners of the Vickers indentation print, without the formation of cone cracking or surface detachment due to shallow lateral cracking [11]. In the case of 9/1 and 8/2 vitreous products, the load was 0.2 N and for 7/3 was 0.9 N. Fracture toughness could not be quantitatively measured, since in all devitrified products, cracking is highly anisotropic. However, the crack propagation mode was studied in order to obtain qualitative results.

Results

As-quenched products were single-phase elementally homogeneous glasses. According to EDS measurements, the composition variation of Pb and Si was comparable to the accuracy of the method, namely ±1 at.%. Transmission electron microscopy (TEM) investigation of the as-quenched samples did not reveal any phase separation, as well. All observations showed a featureless matrix, suggesting a vitreous state of matter. Moreover, the corresponding electron diffraction patterns were composed of a diffuse halo around the transmitted beam, which is indicative of amorphous materials. Their vitreous nature was also revealed by the fact that the respective DTA thermographs possessed the characteristic glass transition endotherm. The position of the glass transition temperature (T_g) of G and N products was found at 420 °C for 7/3 and 8/2 vitreous products and at 350 °C for 9/1 vitreous product. The corresponding DTA thermographs are depicted in Fig. 1.

The values of microhardness, elastic constant and fracture toughness of the vitreous products are listed in Table 2. Glass products showed an increase on the values of microhardness and elastic constant with increasing SiO$_2$ content. Fracture toughness of 9/1 is marginally lower than 8/2 vitreous product, taking into account the experimental error, while it significantly increases in the case of 7/3 vitreous product. Thus, addition of silica makes the vitreous network harder, stiffer and tougher. The experimental errors in the case of fracture toughness values can be considered as relatively low, since scattering can reach the 30% of the measured value. This is due to the fact that the indentation induced crack lengths were characterized by high degree of repeatability and isotropic crack
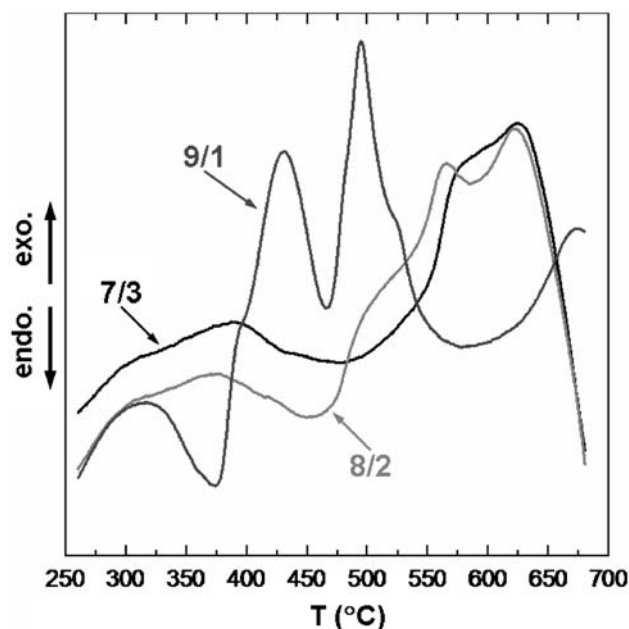
Fig. 1 DTA thermographs for all three starting vitreous products

propagation. The latter means that radial cracks emanate from all four corners of the Vickers indentation print and have nearly identical lengths. Such repeatable cracking may stem from the relatively low fracture toughness of vitreous products that allows a significant portion of the indentation energy to activate crack growth.

Crystallization in the case of 9/1 vitreous product was intense, resulting in a fully crystallized product that cannot be considered as glass-ceramic. It appears that the tendency for devitrification is high enough in the 9/1 batch composition, so as to foster uncontrolled crystallization. From the phase diagram of the PbO–SiO$_2$ system (Fig. 2), we can assume that the ceramic phase present in this product is Pb$_4$SiO$_6$. The devitrification process in the 8/2 and 7/3 compositions occurred in a controlled manner, resulting in glass-ceramic materials with morphologies that are depicted in the optical micrographs containing Vickers indentation prints (Fig. 3). The most probable crystalline phase according to the phase diagram is Pb$_3$Si$_2$O$_7$ in both cases. The separated crystallites in the case of 8/2 crystallized product are randomly oriented oblong parallelograms, while

Table 2 Mechanical properties of vitreous and resulting glass-ceramic products

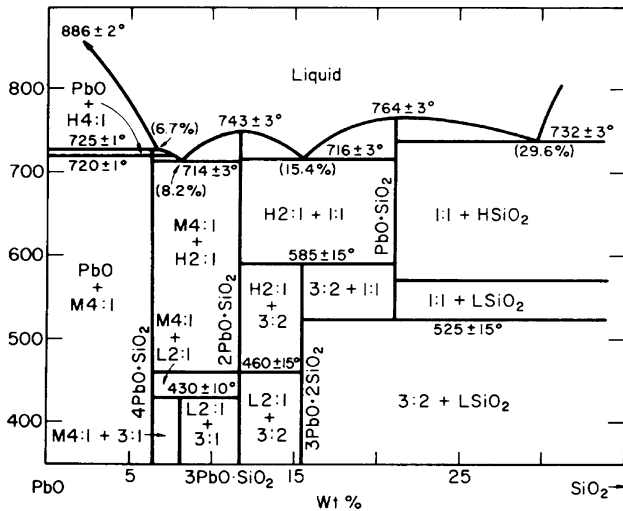| Code name	Vitreous products			Glass-ceramic products		
	H_K (GPa)	E (GPa)	K_{IC} (MPa m$^{1/2}$)	H_K (GPa)	E (GPa)	Fracture mode
9/1	2.03 ± 0.02	7.12 ± 0.08	0.11 ± 0.003	2.73 ± 0.11	9.57 ± 0.43	Transgranular
8/2	2.30 ± 0.08	8.04 ± 0.26	0.13 ± 0.007	1.95 ± 0.22	N.A.[a]	Intergranular
7/3	2.87 ± 0.05	9.94 ± 0.20	0.20 ± 0.007	2.77 ± 0.14	9.73 ± 0.51	Mixed

[a] Not applicable

Fig. 2 Binary phase diagram of PbO–SiO$_2$ system, at the high PbO region

in 7/3 crystallized product they have the form of needles. These crystalline needles form small areas where they are oriented parallel to each other.

The microhardness value of 9/1 product increased after devitrification. This behaviour is quite common, since crystalline matter is in most cases harder than amorphous. In the case of 7/3, devitrification does not have any measurable effect on the microhardness value, while in the case of 8/2, devitrification seems to result in a decrease in the microhardness value. It should be noted though that the experimental error in the last case is significant. Increase in

the number of microhardness measurements did not reduce the experimental error, so the source of uncertainty in the measurement is poor repeatability, i.e. it is inherent in the 8/2 glass-ceramic. As a result, it would be more appropriate to say that the microhardness value is marginally decreased after devitrification in this case.

The most interesting property in the glass-ceramic products is the crack propagation pattern. In the case of 9/1 ceramic product straight propagation of the indentation induced cracks manifests transgranular fracture. Glass-ceramic 8/2 shows a typical intergranular fracture with cracks following an irregular serrate path. In this case, the cracks do not emanate only from the corners of the indentation print. Finally, glass-ceramic 7/3 shows a mixed fracture mode. This mode of fracture has been reported previously in the literature in the case where thin needle-like crystallites have been separated [2].

The measured microhardness values and elastic constants as well as the observed active fracture modes of all thermally treated vitreous samples are depicted in Table 2.

Discussion

Starting vitreous products were homogeneous with respect to their elemental composition. This is due to the fact that the batch materials were mixed and mechanically milled and that the heating temperature was significantly higher than the liquidus temperature, fostering interdiffusion of the constitutive elements. Product 9/1 was vitreous, despite
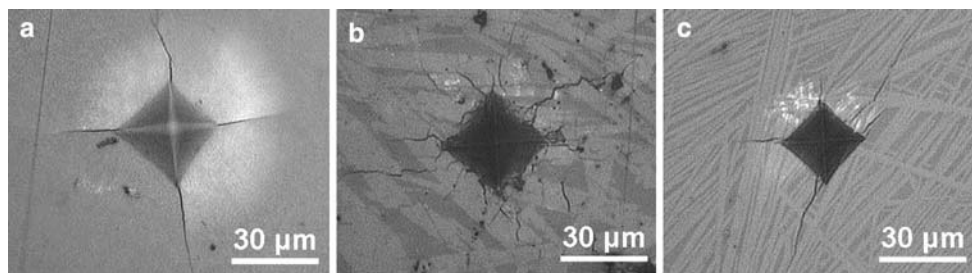

Fig. 3 Optical micrographs illustrating the morphology of the three devitrified products: (**a**) 9/1 product was fully crystallized exhibiting a featureless background; (**b**) and (**c**) separated crystallites (brighter areas) within a vitreous matrix in 8/2 and 7/3 products, respectively. All optical micrographs contain Vickers indentation prints, used to obtain the fracture toughness of the products

the high PbO concentration. This arises from the fact that the samples were relatively small; in such cases in PbO–SiO_2 binary system glass can be formed for PbO content up to 92 wt.% [12]. In other batch compositions, glasses can be easily formed.

Vitreous products 7/3 and 8/2 were devitrified in a controlled manner and the resulting products can be considered as glass-ceramics [13]. However, 9/1 devitrified product was transformed into a fully crystallized material, i.e. a ceramic product. This can be interpreted by considering that this product is marginally within the glass-making compositional area, as it has been already mentioned. This can also be seen by the significantly small temperature interval between the glass transition and the devitrification exotherms (T_{exo}) that is 70 °C. For comparison, in 7/3 and 8/2 products, the temperature interval is approximately 130 °C, almost twice as wide. It is well known that a vitreous material with narrow temperature interval between T_g and T_{exo} presents lower thermal stability than another one with wider temperature interval [14].

It has been obtained that decrease in PbO content results in an increase in microhardness, elastic constant and fracture toughness, in vitreous products. This is in accordance with the structural changes of the vitreous network due to the increasing content in silica. Since in all cases the content in lead is higher than 40 mol%, the three-dimensional extended vitreous network is built from PbO_4/PbO_3 structural units that are connected with Q_2 and Q_1 depolymerised SiO_4 units [7, 15]. Increase in the silica content increases the content in more rigid Si–O–Si bonds, since the content in Q_1 and Q_2 units is increased. Q_1 and Q_2 structural units contain one and two Si–O–Si bonds, or bridging oxygen atoms, respectively. This interprets the observed increase in the abovementioned parameters. In order to form an indentation or to produce a propagating crack three physical mechanisms should be considered. Plastic flow and to a lesser degree densification, for the former, and generation of new free surfaces for the latter [16, 17]. All three mechanisms require the rupture of atomic bonds. As a result, a vitreous network with higher content in Q_1 and Q_2 units is less susceptible to plastic deformation or fracture. In Fig. 4, a schematic representation of Q_i units, where i is the number of bridging oxygen atoms is depicted.

The significant experimental uncertainty in the measurement of microhardness in 8/2 devitrified product is not a matter of improperly obtained measurements, but is due to poor repeatability. This is caused from the easily formed microcracks at the edges of Knoop indentation prints. It has been reported that microcracking can affect the size of the indentation print, and as a result the obtained microhardness value [18]. Consequently, the observed higher
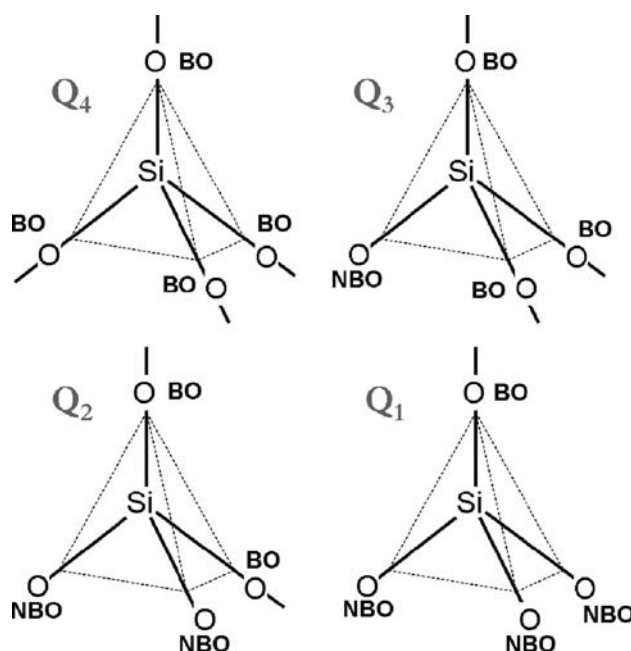
Fig. 4 Schematic representation of Q_i units, where the positions of bridging (BO) and non-bridging oxygen (NBO) atoms are shown

uncertainty reflects the microcrack formation. This also explains the inability to obtain the elastic constant, since measurement of the length of the smaller diagonal of the Knoop indentation print is highly inaccurate.

In 7/3 product, the crack propagation pattern depends on the orientation of the crack with respect to the longer dimension of the crystallites. When the crack propagates parallel to the longer dimension, it follows the crystallite/amorphous matrix interface, i.e. the propagation is intergranular. When the crack propagates at right angles it ruptures the crystallites, i.e. the propagation is transgranular. This is because of their relatively small width, namely 1–1.5 μm. This order of width has been observed in other cases to promote transgranular fracture [5]. As a result, a mixed crack propagation mode is observed in this case.

In the case of 8/2 devitrified product, the cracks deviate from straight-line propagation. This is a typical behaviour of a material with high toughness. The length of the cracks may be longer, but the extent of the damage (the distance of the crack tip from the indentation that produces it) is confined inside a smaller area. If there was a need to decide which of the two products should be used as armour, for example, 8/2 product would be the most appropriate.

Although the crystallites in the two above cases have the same composition, they show a different crack propagation pattern. This can be interpreted by the difference of the shape and mean size of the crystallites. The crystalline needles in the 8/2 devitrified product are thicker (most of them are wider than 10 μm), while in the 7/3 are thinner than 3 μm. This is in agreement with the literature [2, 5],

where it has been reported that increase in the thickness of oblong crystallites results in a shift from transgranular to intergranular fracture.

Devitrified 9/1 product shows a clear transgranular fracture mode. This is an indication of a ceramic material with strong interfaces, i.e. of grain boundaries with strong cohesion. The mechanical properties though cannot be directly compared with those of the glass-ceramic products. The difference in the fracture mode can be due to the different crystalline phase that has been separated, but the absence of amorphous phase, in the devitrified 9/1 product, cannot be neglected. Especially, in the present case where lead oxide, which has not drawn the same scientific interest as silica, plays a dominant role as a glass former. It seems that glasses made of lead oxide have the ability to absorb indentation energy, when they form the residual vitreous matrix in a glass-ceramic material, in a more efficient way compared to silica based matrices. However, this is a matter of further investigation.

A novel method for the measurement of fracture toughness has been recently published [19]. In this method, the fracture toughness value is calculated from the derivation of its interrelation with a critical load PF. This critical load is the indentation load needed for edge chip formation for indentations located at prescribed distances from the edges of materials that are characterized by a single-valued toughness, for example homogeneous glasses and fine-grained polycrystalline ceramics. This method would be rather useful in the present case because the fracture toughness value of the glass-ceramics could be derived, without the need of isotropic radial crack formation. However, the micro-indenter used is the present study cannot apply high enough loads for edge chip formation in the above materials and as a result it cannot be applied.

Conclusions

The active fracture modes in ceramic and glass-ceramic materials, devitrified from rich in PbO vitreous products were examined. The mechanical properties of the parent vitreous products were affected by the content in PbO.

Decrease in PbO content resulted in an increase in the microhardness, elastic constant and fracture toughness. This was attributed to the increase in the content of Q_1 and Q_2 SiO_4 structural units. The modes of fracture in the 8/2 and 7/3 devitrified products were affected by the width of the separated crystallites, in accordance with previously published works in silicate based glass-ceramics; decrease in the width of $Pb_3Si_2O_7$ crystallites resulted to a shift in the fracture mode from intergranular, in devitrified 8/2 product, to mixed, in devitrified 7/3 product.

References

1. Hölland W, Beal G (2002) Glass-ceramic technology. ACS, Westerville, p 4
2. Kavouras P, Charitidis C, Karakostas Th (2006) J Non-Cryst Sol 352:5515
3. Kriven EM, Lee SJ (2005) Am J Ceram Soc 88:1521
4. Zhai H, Huang Y, Wang C, Wu X (2000) J Am Ceram Soc 83:2006
5. Charitidis C, Karakasides TE, Kavouras P, Karakostas Th (2007) J Phys Condens Mat 19:266
6. Shelby JE (1997) Introduction to glass science and technology. RSC Paperbacks, Cambridge, p 78
7. Wang PW, Zhang L (1996) J Non-Cryst Sol 194:129
8. Anstis GR, Chantikul P, Lawn BR, Marshall DB (1981) J Am Ceram Soc 64:533
9. Amin KA (2000) Engineered materials handbook: ceramics and glasses. ASM International, p 599
10. Marshall DB, Noma T, Evans AG (1982) J Am Ceram Soc 65:C175
11. Cook RF, Pharr GM (1990) J Am Ceram Soc 73:787
12. Vogel W (1994) Glass chemistry, 2nd edn. Springer-Verlag, p 158
13. Strnad Z (1986) Glass-ceramic materials. Elsevier, Amsterdam, p 230
14. Hrubý A (1972) Czech J Phys B 22:1187
15. Shrikhande VK, Sudarsan V, Kothiyal GP, Kulshreshtha SK (2001) J Non-Cryst Sol 283:18
16. Doremus RH (1994) Glass science and technology. John Wiley and Sons, New York, p 163
17. Salama SN, El-Batal HA (1994) J Non-Cryst Solids 168:179
18. Li H, Bradt RC (1996) J Mater Sci 31:1065
19. Chai H, Lawn BR (2007) Acta Mater 55:2555